European Journal of Pharmaceutics and Biopharmaceutics 71 (2009) 243–250

Contents lists available at ScienceDirect

European Journal of Pharmaceutics and Biopharmaceutics

journal homepage: www.elsevier.com/locate/ejpb

Research paper

Nanoparticles for skin penetration enhancement – A comparison of a dendritic core-multishell-nanotransporter and solid lipid nanoparticles

Sarah Küchler [a], Michal R. Radowski [b], Tobias Blaschke [c], Margitta Dathe [d], Johanna Plendl [e], Rainer Haag [b], Monika Schäfer-Korting [a,*], Klaus D. Kramer [c]

[a] Institut für Pharmazie, Freie Universität Berlin, Berlin, Germany
[b] Institut für Chemie und Biochemie, Freie Universität Berlin, Berlin, Germany
[c] Institut für Physik, Freie Universität Berlin, Berlin, Germany
[d] Leibniz-Institut für Molekulare Pharmakologie, Berlin, Germany
[e] Institut für Veterinär-Anatomie, Freie Universität Berlin, Berlin, Germany

ARTICLE INFO

Article history:
Received 17 April 2008
Accepted in revised form 7 August 2008
Available online 30 August 2008

Keywords:
Dendritic core-multishell nanotransporters
Solid lipid nanoparticles
Skin penetration
Cellular uptake
Nile red

ABSTRACT

Nanosized particles are of growing interest for topical treatment of skin diseases to increase skin penetration of drugs and to reduce side effects. Effects of the particle structure and size were studied loading nile red to dendritic core-multishell (CMS) nanotransporters (20–30 nm) and solid lipid nanoparticles (SLNs, 150–170 nm).

Interaction properties of CMS nanotransporters with the dye molecules – attachment to the carrier surface or incorporation in the carrier matrix – were studied by UV/Vis and parelectric spectroscopy. Pig skin penetration was studied *ex vivo* using a cream for reference. Interactions of SLN and skin were followed by scanning electron microscopy, internalisation of the particles by viable keratinocytes by laser scanning microscopy.

Incorporating nile red into a stable dendritic nanoparticle matrix, dye amounts increased eightfold in the stratum corneum and 13-fold in the epidermis compared to the cream. Despite SLN degradation at the stratum corneum surface, SLN enhanced skin penetration less efficiently (3.8- and 6.3-fold). Viable human keratinocytes showed an internalisation of both nanocarriers.

In conclusion, CMS nanotransporters can favour the penetration of a model dye into the skin even more than SLN which may reflect size effects.

1. Introduction

Due to the lower risk of systemic side effects, topical treatment of skin diseases appears favourable. Yet the stratum corneum counteracts the penetration of xenobiotics into viable skin, and only a few percent of the applied drug is absorbed. Particulate carrier systems can improve dermal penetration [1]. Since skin lipids greatly contribute to the penetration barrier, lipid carriers, which may allow lipid exchange with skin surface, appear very promising. These are liposomes [2,3], solid lipid nanoparticles (SLNs), nanostructured lipid carriers (NLCs), lipid microspheres [1,4], microemulsions [5], and hexagonal phase nanodispersions [6] attaching themselves to the skin surface. Indeed, the nature of the lipid particle and the mode of drug interaction with the lipid matrix proved relevant [7]. SLN can enhance the skin penetration of drugs and the dye nile red more than NLC and microspheres [8,9]. Especially when the drug is located at the particle surface, SLN can also induce epidermal targeting [9,10]. Although tretinoin absorption was not influenced by loading to SLN, tolerability was improved [11]. Also liposomes enhancing tretinoin uptake [12] reduce local side effects [13]. This is also seen with triamcinolone acetonide and skin thinning – which is the most relevant side effect after the long-term topical application of potent glucocorticoids [14] – is therefore less severe [15].

Besides lipid nanoparticles, polymer particles can enhance dermal uptake or improve tolerability as described for benzoyl peroxide [16,17], fluorouracil [18] and once more for nile red [19]. Currently, however, polymer particles are only rarely studied for

Abbreviations: ABU, arbitrary brightness unit; CMS, dendritic core-multishell; $\Delta\varepsilon$, dipole density; f_0, dipole mobility; FITC, fluorescein isothiocyanate; KBM, keratinocyte basal medium; LD, laser diffractometry; LSM, laser scanning microscope/microscopy; NLC, nanostructured lipid carrier(s); PBS, phosphate buffered saline; PCS, photon correlation spectroscopy; PEE, penetration enhancing effect; PG, polyglycerol amine; PI, polydispersity index; PS, parelectric spectroscopy; SE, standard error of the mean; SEM, scanning electron microscopy; SLN, solid lipid nanoparticle(s); r.t., room temperature.

* Corresponding author. Institut für Pharmazie der Freien Universität Berlin, Königin-Luise-Str. 2-4, D-14195 Berlin, Germany. Tel.: +49 30 838 53283; fax: +49 30 838 54399.
E-mail address: msk@zedat.fu-berlin.de (M. Schäfer-Korting).

0939-6411/$ - see front matter © 2008 Elsevier B.V. All rights reserved.
doi:10.1016/j.ejpb.2008.08.019

topical application yet have gained special interest due to their potential for drug targeting in tumor therapy [20]. Nanosized polymeric carriers are of well controllable sizes and surface polarity [20–22], allowing adaptation to the intended target. Dendritic core-multishell (CMS) nanotransporters can be build up from hyperbranched polymeric cores composed of polyglycerol surrounded by a double-layered shell consisting of a C_{18}-alkyl chain and of monomethoxy poly(ethylene glycol). Above a critical concentration, single nanocarriers with sizes of 8–9 nm form larger aggregates too, with the diameters of 20–50 nm. These supramolecular aggregates can encapsulate lipophilic as well as hydrophilic agents and transport them into polar as well as nonpolar environments [20,21].

In order to determine the influences of the nature and size of nanocarriers on dermal uptake of the loaded agent, we compared the skin penetration of nile red loaded to dendritic nanotransporters and SLN and studied the fate of SLN when applied to the skin. Moreover, we investigated the cellular uptake of both types of nanocarriers by human keratinocytes, since the internalisation of particles may become relevant with damaged skin. To our best knowledge, lipid carriers and dendritic core-multishell carriers have not yet been compared.

2. Materials and methods

2.1. Materials

Compritol® 888 ATO (glyceryl behenate) was a gift from Gattefossé (Weil a. Rh., Germany), oil-in-water cream (as described by the "Deutscher Arzneimittelcodex 2004" containing: glycerol monostearate 60 4.0 g, cetylalcohol 6.0 g, medium chain triglycerides 7.5 g, white vaseline 25.5 g, macrogol 20-glycerolmonostearate 7.0 g, propylenglycol 10.0 g, water 40.0 g) was supplied by Caelo (Hilden, Germany). The emulsifier Lutrol F68® (Poloxamer 188) was obtained from BASF (Ludwigshafen, Germany). Nile red was obtained from ABCR (Karlsruhe, Germany) and Sigma–Aldrich (Munich, Germany). Sodium azide, 2-desoxy-D-glucose, formaldehyde, ethanol, methanol, fatty acid free bovine serum albumin (BSA), reagents and media, except where noted, were purchased from Sigma–Aldrich (Munich, Germany). 1,18-octadecanoic acid was obtained from Cognis (Langenfeld, Germany). Chemicals for the synthesis of the CMS nanotransporters were purchased from Fluka (Seelze, Germany), except polyglycerol amine (PG_{10000}) which was prepared according to the published procedures [21,23,24].

Pig skin of the axillary region from donor animals (breed: "Deutsche Landrasse, 45–55 kg, 8–12 weeks old) was provided by the Department of Comparative Medicine and Facilities of Experimental Animal Sciences, Charité (Berlin, Germany). Immediately after withdrawal, the skin was placed in an ice-cold cloth and transferred to the laboratory taking care to avoid any contamination of the skin surface by lipids of the subcutis. In the laboratory subcutaneous tissue was removed and the skin was stored at a temperature of −20 °C for up to 6 months [25].

Human keratinocytes were isolated from juvenile foreskin and cultivated as described elsewhere [26]. Cells were grown in keratinocyte basal medium supplemented with epidermal growth factor, insulin, gentamicin sulphate, amphotericin B, hydrocortisone and bovine pituitary extract (KBM) which were purchased from Lonza (Walkersville, MD, USA).

2.2. Particle preparation

SLNs, composed of 10% solid lipid (Compritol® 888 ATO), 0.004% dye and 2.5% emulsifier, were prepared as described [8]. In short, nile red was dissolved in melted lipid at 95 ± 5 °C. An aqueous solution of Poloxamer 188® of the same temperature was added and a pre-emulsion was formed using an ultra turrax. The premix was homogenized by an Emulsiflex C5 high pressure homogenizer (Avestin, Mannheim, Germany) at 500 bar for 2.5 min. SLNs were stored at 8 °C and used for penetration experiments within 1 month after preparation, though stable for almost 3 months [8].

The CMS nanotransporters have the empirical formula $PG_{10000}(-NH_2)_{0.7}(C_{18}mPEG_6)_{1.0}$ (Fig. 1). Polyglycerolamine [23] and 1-(2,5-dioxopyrrolidin-1-yl)-18-methoxy-poly(ethylene glycol)yl octadecanedioate [21] were synthesized using the previously published procedures. Polyglycerolamine was dissolved in methanol and a solution of 1-(2,5-dioxopyrrolidin-1-yl)-18-methoxy-poly(ethylene glycol)yl octadecanedioate in methanol was added dropwise. The reaction mixture was stirred for 24 h at room temperature and then concentrated in vacuum. The obtained crude product was dissolved and dialyzed in methanol to give, after drying under vacuum, a solid product.

For nile red (0.004%) encapsulation, $PG_{10000}(NH_2)_{0.7}(C_{18}mPEG_6)_{1.0}$ was dissolved in water, the dye was added and the obtained suspension was vigorously stirred for 72 h. Afterwards it was filtrated to remove any traces of insoluble residues of nile red.

2.3. Particle characterisation

Photon correlation spectroscopy (PCS, Malvern Zetasizer ZS, Malvern Instruments, Malvern, UK) was used for particle size characterisation of the SLN and the CMS nanotransporters to evaluate the mean particle size (*z*-average) and the polydispersity index (PI) as a degree for the width of the distribution. Larger particles with micrometer size were detected by laser diffraction (LD, Coulter LS 230, Miami, FL [4]).

To follow the loading and diffusion process of nile red to the CMS nanotransporters, UV/Vis spectra were recorded on a Scinco S-3150 spectrometer (range: 187–1193 nm; resolution: 1024 points). Calibration was performed at 360.85 nm and 453.55 nm with holmium oxide glass. All spectra were recorded at room temperature and evaluated with the programs LabPro® Plus (Scinco Co., Ltd., Groß-Umstadt, Germany), Microsoft® Excel 2000 (Microsoft Corporation), and Origin® 7.0 (OriginLab Corporation, Northampton, MA, USA).

The mode of interaction of nile red molecules and CMS nanotransporters was studied by parelectric spectroscopy (PS). PS allows to measure dipole density $\Delta\varepsilon(c)$ and mobility frequency $f_0(c)$ of the CMS nanotransporters as a function of increasing nile red concentrations c (0–0.004%). The experimental PS set-up consisted of a frequency analyzer (type ZVR, Rohde & Schwarz, München, Gemany) with a notebook for the transmitter steering and data evaluation. Parelectric dispersion $\varepsilon'(f,c)$ and absorption $\varepsilon''(f,c)$ were recorded, each of the curves containing 200 logarithmically equidistant frequency points f in the range $f = (0.1 \ldots 100)$ MHz. Dipole density $\Delta\varepsilon(c)$ and mobility frequency $f_0(c)$ were extracted from these 400 values. Both $\Delta\varepsilon(c)$ and $f_0(c)$ have different characteristics for the cases of agent attachment (non-covalently bond) to the surface or incorporation into the carrier matrix and thus allow a clear distinction [27]. The underlying theoretical model has been successfully applied before to various lipid nanocarriers and is described elsewhere [10]. In particular, it has been used to show

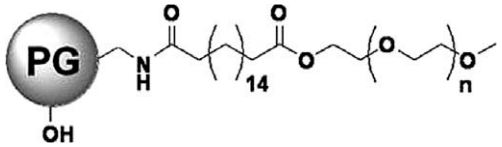

Fig. 1. Chemical structure of the dendritic core-multishell nanotransporters

that nile red is incorporated into the lipid matrix of SLN [8,27]. Interestingly, the dependence of the concentration c of the dye on the diffusion time t is a monotonously increasing, nonlinear function, which allows to connect both quantities by the relation $c = c(t)$. Furthermore, the dye loading to the CMS nanotransporters was studied by UV/Vis measurement.

2.4. Nile red loaded cream

Nile red cream 0.004% [8] served as a reference in the skin penetration studies. The dye dispersed in some paraffin oil droplets was incorporated into base cream. The cream was stored at 8 °C.

2.5. Skin penetration

For characterization of the nile red penetration, the fluorescence intensities of stratum corneum, viable epidermis and dermis were evaluated by validated test procedures for the Franz cell set-up [25,28] and picture analysis [8]. CMS nanotransporters, SLN and cream were tested in parallel using skin of the same donor animal ($n = 4$) [1,25]. On the day of the experiment, pig skin was thawed and 1000 ± 100 μm skin sheets were prepared using a Dermatome™ (Aesculap, Tuttlingen, Germany). Punched discs of 2 cm diameter were mounted to static-type Franz cells (diameter 15 mm, volume 12 ml, PermeGear Inc., Bethlehem, PA, USA) with the horny layer facing the air and the dermis having contact with the receptor fluid phosphate buffered saline pH 7.4 (PBS; 33.5 °C, skin surface temperature about 32 °C) stirred at 500 r/m. After equilibration for 30 min, 35 μl of the test formulations was applied onto the skin surface (finite-dose approach) and remained there for 6 h, sealing the donor compartment with Nescofilm®. Then the skin was removed from the Franz cells, and surplus formulations were gently removed by carefully washing the skin using PBS. Subsequently, treated skin areas were punched, embedded in tissue freezing medium (Jung, Nussloch, Germany) and stored in Peel-Aways® (Polyscience, Eppelheim, Germany) at a temperature of −80 °C.

For fluorescence reading, the skin discs were cut into vertical slices of 20 μm thickness using a freeze microtome (Frigocut 2800 N, Leica, Bensheim, Germany). Slices were stored at +4 °C and analysed within 24 h, then subjected to normal light and fluorescence light. Nile red amounts in the stratum corneum, viable epidermis and dermis were determined using an inverted fluorescence microscope (20× magnification, Axiovert 200, Zeiss, Jena, Germany) equipped with a monochrome camera (AxioCam HR, version 5.05.10, Zeiss). Exciting the samples at 546 nm and setting the camera integration time to 10 ms, fluorescence recorded in the red band (beam splitter wavelength 585 nm) was quantified by image analysis software (Axiovision 3.1.3.1, Zeiss). The integration of arbitrary pixel brightness values (ABU) gives the relative dye content within the randomized areas located in the stratum corneum, epidermis and superficial dermis (100 μm below the basal membrane). Pixel intensities were corrected by subtracting background fluorescence intensity units obtained from the measurement of the native fluorescence of the respective skin layers of untreated skin (mean values of 3 skin samples). The respective background levels are stratum corneum 165 ABU, viable epidermis 160 ABU and dermis 55 ABU. Corrected ABU values are reported.

2.6. Interactions of SLN and skin

To study the interactions between SLN and skin by scanning electron microscopy pig skin (2 donor animals) was prepared as described above and transferred to 6-well plates (TPP, Trasadingen, Switzerland) with cell culture inserts (Nalge Nunc International, Wiesbaden, Germany). Dulbecco's modified Eagles medium Nutrient Mixture F12 Ham® (DMEM; PAA Laboratories, Pasching, Austria) was used for nourishing the skin via the dermal compartment. SLNs were applied on the skin surface, incubated at 32 °C and left in place for 0.5, 2 or 4 h. Then the skin was removed, conserved in Karnovsky solution and postfixed in 1% osmium tetroxide solution (Chempur, Karlsruhe, Germany). The tissue was dehydrated in an ascending ethanol series for 10–30 min, treated twice with hexamethyldisiliazane (HMDS, Ted Pella Inc., Redding, CA, USA) for 15 min and air-dried over night. After fixation with fluid carbon dioxide, the samples were dried under vacuum condition for 24 h. Finally, skin surface sputtered with gold (layer thickness 40–45 nm, SCD 050 Sputter Coater, Bal-Tec, Balzers, Liechtenstein) was visualized with DSM 950 (Zeiss, Oberkochen, Germany).

2.7. Cellular uptake

Primary human keratinocytes of the first or the second passage were grown to a confluence of about 70%, washed with PBS and trypsinated. DMEM with 10% FCS was added and the cell suspension was centrifuged at 1000 rpm and 4 °C for 5 min. Cells were resuspended in PBS and counted.

For laser scanning microscopy (LSM), 2×10^4 keratinocytes per well were seeded in 8-well chamber slides (Lab-Tek™ II Chambered Coverglass, Nalge Nunc International, Wiesbaden, Germany). Cells were exposed to SLN and CMS nanotransporters suspended in KBM (suspension stabilised by 1.5% Poloxamer 188) for 0.5 h at 37, 4 °C and under energy depletion. For experiments under energy depletion, cells were pre-treated with a solution of 25 mM 2-desoxy-D-glucose and 10 mM sodium azide in Dulbecco's phosphate buffered saline with calcium and magnesium (PBS wCa^{2+}, Mg^{2+}; PAA Laboratories, Pasching, Austria) for 1 h. The same medium was then used for preparation of the nanocarrier suspensions and as a negative control. KBM served as negative control.

After incubation, medium was removed, cells were washed twice with PBS and surveyed immediately. An invert confocal laser scanning microscope LSM510 (Carl Zeiss MicroImaging, Jena, Germany) was used. Excitation was performed at 543 nm using a helium–neon laser and a dichroitic mirror HFT 543 for wavelength selection. Emission was measured using a cut-off filter LP560. To distinguish between particle adsorption and internalization, a solution of trypan blue (0.4%; w/v) was finally added. Accumulation in the intact cell membrane is registered by a pronounced increase in the fluorescence. Thereby a differentiation of living and dead cells was possible, too. To verify that the fluorescence of the cells is due to the cellular uptake of the SLN and not due to an uptake of the dye which was released from the nanoparticles, control experiments were performed applying the dispersion of SLN into cell inserts (0.02 μm, Nalge Nunc, Wiesbaden, Germany) which separated the lipid nanoparticles physically from the cells. Keratinocytes were observed by LSM [29]. This experimental approach is not possible with CMS nanotransporters which pass through the cell insert because of the smaller size (20–30 nm).

To quantify nile red uptake, 2.5×10^4 keratinocytes per well were seeded into 12-well plates (TPP, Trasadingen, Switzerland), incubated with the test preparations at 4 and 37 °C for 0.5 and 4 h and then washed 8 times with PBS. Following the addition of 400 μl methanol per well, the affiliated amount of nile red was quantified immediately using a microplate reader (FLUOstar Optima, BMG Labtech, Offenburg, Germany), setting the excitation wavelength to 550 nm and emission wavelength to 640 nm (gain 3000, 10 flashes per well/cycle). Each well was aligned three times per measurement and the average was calculated for data evaluation taking native fluorescence of untreated keratinocytes into account.

2.8. Biostatistics

For skin penetration experiments, corrected ABU values obtained from dye uptake following CMS nanotransporters and SLN were related to uptake data from nile red loaded cream. The resulting penetration enhancing effect (PEE) was calculated for all the skin layers of interest (horny layer, viable epidermis, superficial dermis). The PEE of the cream is 1 by definition. The results are presented as average values ± SE obtained from 5 independent experiments (skin from 5 donor pigs). Statistical analysis is based on the H-test of Kruskal and Wallis and subsequently, a post hoc test using X^2-approach. $p \leqslant 0.05$ indicates a difference.

3. Results and discussion

Drug penetration into the skin is often rather poor. This is especially true for the agents of higher molecular mass (>500 Da) [30] and high hydrophilicity [28]. Furthermore, local side effects can be a matter of concern while systemic side effects often are less relevant as compared to oral or intravenous application. Carrier systems, which increase the drug penetration and tolerability are thus of great interest although the systems currently are only at the start of commercial use [4]. Using the lipophilic dye nile red, superiority of SLN over NLC and conventional cream was shown when applying an infinite dose to pig skin *ex vivo* [8]. Moreover, increased nile red delivery from polymer nanoparticles was shown [19,31]. In this study, we investigated the enhancing effect of SLN using the finite-dose approach which is close to the clinical application. Moreover, efficiency of SLN was compared to the efficiency of new dendritic core-multishell nanoparticles (Fig. 1). These appear very interesting for a topical use as lipophilic and hydrophilic molecules can be loaded onto them and the PEG-shell enables the CMS nanotransporters to deliver the loaded agent to polar as well as nonpolar environments [21]. Moreover, the PEG-shell reduces the cytotoxicity of the nanoparticles [22].

3.1. Particle characterization

Particle size and size distribution of the dye-loaded SLN were measured by PCS and LD. PCS measurements showed an average size of 150–170 nm with a polydispersity index of <0.250, respectively. LD measurements confirmed the PCS results. The average size of the CMS structure aggregates was 20–30 nm.

Nile red-loaded SLN incorporate the dye into the lipid matrix [8]. In contrast, nile red loading properties of the CMS nanotransporters have not yet been studied. Evaluation of PS data showed that the dependence of dipole density $\Delta\varepsilon(c)$ and mobility $f_0(c)$ on the nile red concentration c passes extreme values at concentrations around $c = 2.1\ mg_{NE} \times g_{PE}^{-1}$ (Fig. 2). In this relatively small region, the dye molecules are assumed to be non-covalently bound (attached) to the surface of the aggregates and intermolecular cavities. For increasing concentrations, i.e. longer diffusion times during the formulation process, the nile red molecules are assumed to diffuse into the CMS nanotransporters. The intramolecular interaction is visualized by Fig. 3. The validity of this model is well in accordance with the results of UV/Vis measurements taken at a variety of diffusion times t (Fig. 3A). Extraction of the time-dependent amplitudes of both contributions to the UV/Vis spectra reveals the early saturation of the contribution from nile red in hydrophilic surrounding compared to the behavior of the second component representing the lipophilic surrounding (Fig. 3B). The shift in the maximum wavelength (Fig. 3A) is connected to the fluorophore surroundings, due to the change from hydrophilic to lipophilic character with increasing nile red concentration. These findings underline the above given explanation.

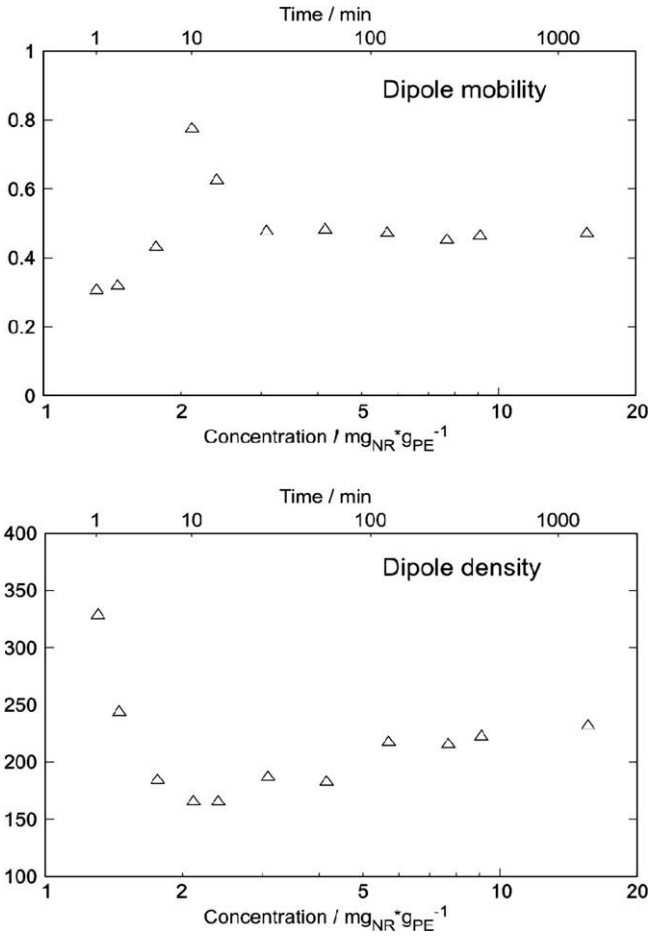

Fig. 2. Dipole mobilities and densities of nile red-loaded dendritic core-multishell nanotransporters for different relative nile red to CMS structure concentrations. For small concentrations, a curved relation between concentration and dipole density (mobility) was obtained, which peaks around a concentration of about $c = 2\ mg_{NE} \times g_{PE}^{-1}$. The two different abscissa scales reflect the dependence $c(t)$ of the concentration c on the diffusion time t which is a monotonously increasing, nonlinear function.

The interpretation, on the basis of the theory of rate processes [32,33], is a pronounced attachment of the dye molecules to the surface of CMS nanotransporters. With increasing nile red concentration, the surface is assumed to be totally clad with the dye molecules. From this concentration on, corresponding to a diffusion time of 10–20 min, nile red diffuses into the agglomerate of the particles occupying first sites between the particles and, with still increasing diffusion time, sites in the matrix of individual particles (Fig. 3). The latter step cannot be followed by the PS method. UV/Vis spectra show that even after a complete coverage of the carrier surfaces, the absorbance with a maximum amplitude at a wavelength of $\lambda = 505$ nm still increases with the increasing nile red concentration. The maximum amplitude at a wavelength of $\lambda = 548$ nm tends towards a steady state value which is reached after a diffusion time exceeding 20 min.

3.2. Cutaneous uptake

Nile red penetration into pig skin has been studied when applying Compritol and Precirol-based SLN, NLC made up of these solid lipids and by using miglyol or oleic acid as liquid lipid, nanoemulsions made from miglyol and from oleic acid as well as nile red loaded oil-in-water cream [8]. Here, we compared the uptake from CMS nanotransporters to the uptake from the most efficient and

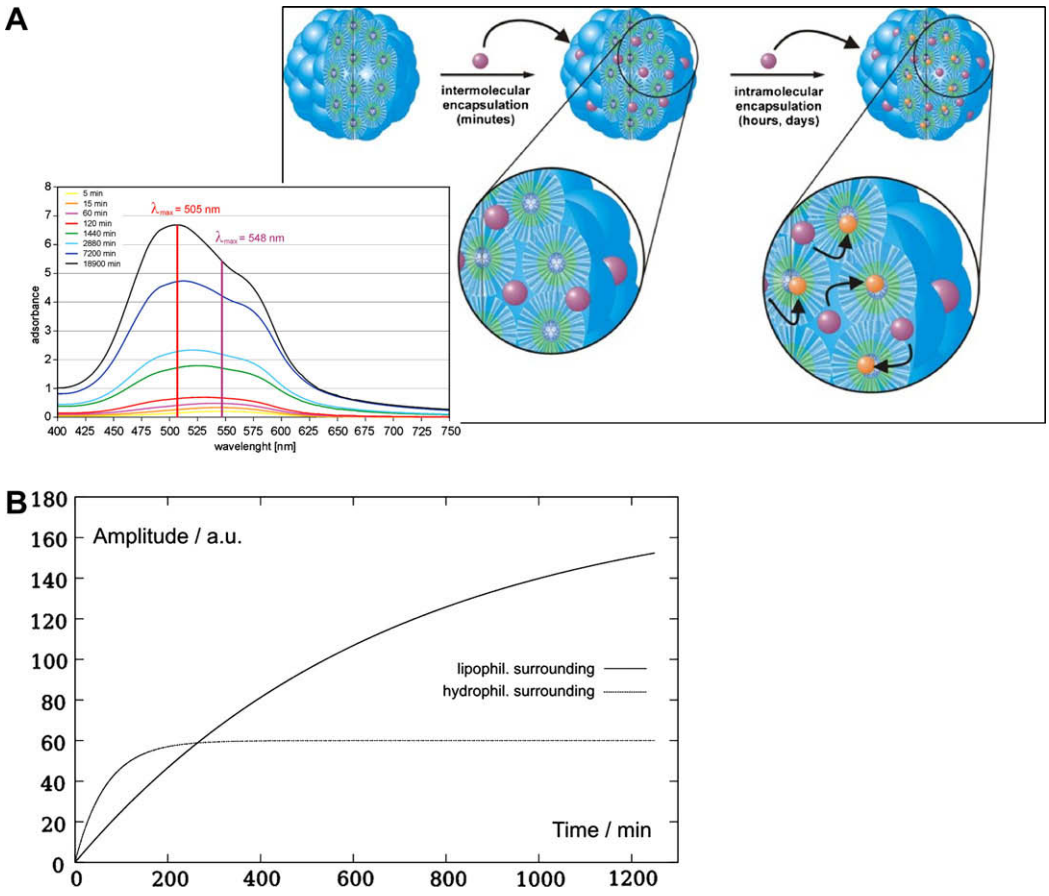

Fig. 3. In the region of small concentrations, nile red is attached to the surface of the aggregates. At higher concentrations, nile red molecules diffuse into the aggregates which is also seen on the basis of the shift of maximum wavelength from 548 to 505 nm as measured by UV/Vis spectroscopy – see inset (A). Time dependence of both contributions to the UV/Vis-spectrum – nile red signal in hydrophilic surrounding as thin line, nile red signal in lipophilic surrounding as thick line – reveals an early saturation onset for the attached molecules and a still increasing contribution for the incorporated molecules (B).

stable SLN dispersion as well as the cream. All preparations contained nile red at the identical concentration of 0.004%. Application conditions were changed from the infinite-dose approach to the finite-dose approach which is closer to the use of topical dermatics in the therapy of skin diseases. Fig. 4A–C shows representative fluorescence microscopy pictures of the vertical pig skin slices obtained after a contact time of 6 h. As to be expected, fluorescence is fading from stratum corneum towards the deeper skin layers with any preparation. The fluorescence pictures already indicate an enhanced dye penetration into the different skin layers when applying the nanocarriers as compared to the cream. Corrected arbitrary pixel brightness values of the skin sections give more detailed information (Fig. 4D). Loaded to SLN, dye penetration increased about fourfold compared to the cream ($p \leqslant 0.05$). This holds true when using both the finite- and the infinite-dose approach [8]. Nile red loading to CMS nanotransporters enhanced the uptake about eightfold in the stratum corneum and even up to 13-fold in viable epidermis. The increase in nile red stratum corneum penetration by loading to CMS nanocarriers significantly exceeded the uptake from cream and for SLN. Moreover, nile red amounts in viable epidermis and superficial dermis were significantly higher following the CMS nanotransporters as compared to the cream ($p \leqslant 0.05$). A major improvement in skin penetration was also seen by loading nile red to biodegradable poly(ε-caprolactone) nanoparticles [31]. Moreover fluorescein isothiocyanate and ciclosporin A uptake by the skin increased twofold when applying a hexagonal phase nanodispersion as compared to a hydroalcoholic solution and a solution in olive oil [34].

The superiority of penetration enhancement by CMS nanotransporters over SLN may result from the smaller size of the polymeric particles (20–30 nm) as compared to the lipid particles (150–170 nm), which then even surmounts the expected effects of lipid exchange. Accumulation of the nanoparticles within the furrows between the corneocytes can facilitate dye transport towards deeper skin layers [19]. This holds true both for CMS nanotransporters and SLN. By freeze-fracture transmission electron microscopy we know that Compritol-based SLNs are shaped like platelets [35,36], which supports intense contact with the skin lipids and the sliding of SLN between the superficial corneocytes. Thus, we next tested our hypothesis that SLN platelets may deliver the loaded substance by an interaction of the lipid building up the particles, and skin surface lipids. Indeed, scanning electron microscopy results indicate a pronounced change of the lipid particles over the time when having contact with the skin surface (Fig. 5). Thirty minutes after application, SLN spread over the skin surface were consistently detected in all viewed parts of the skin. Two hours after application, some of the SLN had lost their primary shape and seemed to have melted. Moreover, the number of visual nanoparticles had declined. After 4 h, SLNs were only found sporadically and SLNs were not detectable in many surveyed areas. This result supports our hypothesis of the mechanism of drug delivery to the skin, which is a mixing of the lipids of particle and skin surface. Moreover, SLN can enhance skin penetration also by occlusion, a high degree of crystallinity (95%) is of great importance [37]. If the polyethylenglycol shell of the CMS nanotransporters, which has the property to adapt within hydrophilic as well as

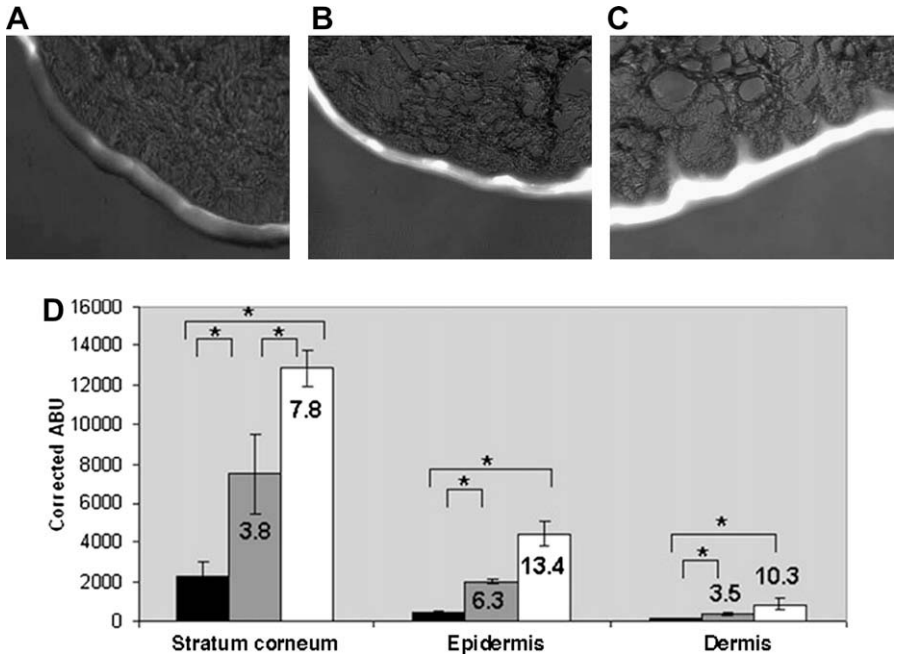

Fig. 4. Staining of pig skin ($n = 4$ donor animals) following the application of 0.004% nile red loaded cream (A), SLN (B) and CMS nanotransporters (C). The pictures are obtained by superposing normal light and fluorescence images of the same area. (D) The arbitrary pixel brightness values (ABU) corrected for background fluorescence (cream, black columns; SLN, grey columns; CMS nanotransporters, white columns) are presented. The inserted numbers give the respective enhancement of penetration over cream (PEE), *differences ($p \leqslant 0.05$).

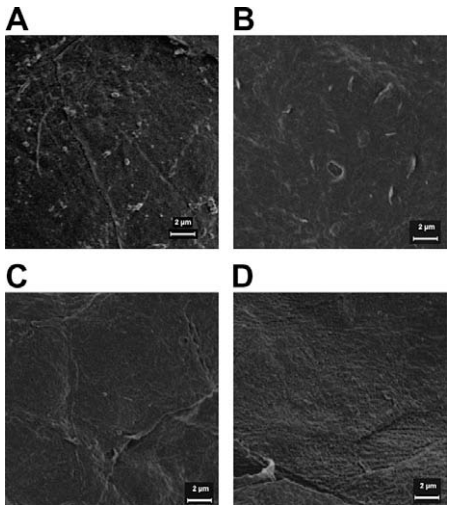

Fig. 5. Interaction of SLN and skin surface. SLN dispersion was applied to the skin of a single donor pig for 0.5 h (A), 2 h (B) and 4 h (C), respectively (skin surface temperature: 32 °C). (D) Untreated pig skin is shown. Representative SEM pictures (magnification 5000×). The same result was obtained when using the skin of the second donor pig.

lipophilic environments, favours drug delivery to the skin as described for bio-adhesive layer systems [38] needs future investigation. Particle size is too small to be detectable by SEM. Yet the improved skin penetration of the dye from the CMS nanocarrier is well explained by its smaller size (20–30 nm) and thus a higher ratio of particle surface and volume facilitating dye release.

Moreover, polymeric nanoparticles 20 and 200 nm in size labelled by covalent binding of fluorescein isothiocyanate (FITC) accumulate in skin appendages [31] and for particles of 750 nm to 10 μm in size, a preferred dye uptake via hair follicles was described [39,40]. SLN and CMS nanotransporters penetrating to the orifices of porcine hair follicles and releasing the dye into the deeper strata may contribute to an enhanced dye penetration of pig skin. Our results do not indicate that intact nanoparticles penetrate into the horny layer.

Epidermal targeting of drugs attached to SLN surfaces [9,10,41] and loaded to liposomes build up from epidermal lipids [42] as well as to transfersomes [15] is possible. No targeting effect was seen for SLN and CMS carriers in this study, which is well in accordance with the incorporation of nile red into the lipid matrix of SLN [8] and the CMS nanotransporters (Figs. 2 and 3).

3.3. Cellular uptake

Since intact nanoparticles can have contact with viable keratinocytes when applied to injured skin, we next studied if keratinocytes may take up SLN and dendrimers as previously shown for liposomes [43,44]. Cellular uptake of nanoparticles including SLN by various cell types has been already described [34,45–47]. This holds true especially with respect to cancer cell lines like human cervix carcinoma cells [45] and human breast carcinoma cells [47], which offer new approaches of the carriers as tumor therapeutics.

Cellular uptake of fluorescent-labelled SLN and CMS nanotransporters was detected by LSM. Differences concerning the uptake of both were not seen. Already, after 0.5 h of incubation at 37 °C fluorescence was detectable in the cytoplasm of the keratinocytes, but not in the nucleus (Fig. 6A and B). Particles accumulate with time, although more than 50% of the fluorescence intensity measured after 4 h is already attained at 0.5 h. Only a very weak fluorescence was detectable by LSM, when the SLNs were separated physically from the cells. Therefore, fluorescence after incubation with SLN is due to the particle uptake and not to a staining by a released dye. The highly solvent-dependent fluorescence of nile red and its rapid fading in hydrophilic environments [48] exclude dye release experiments with both nanoparticulate systems. Yet, nile red encapsulation by the particles should retard dye release and in all probability the fluorescence after application of the CMS, too, is a result of cellular uptake and not of a staining by released

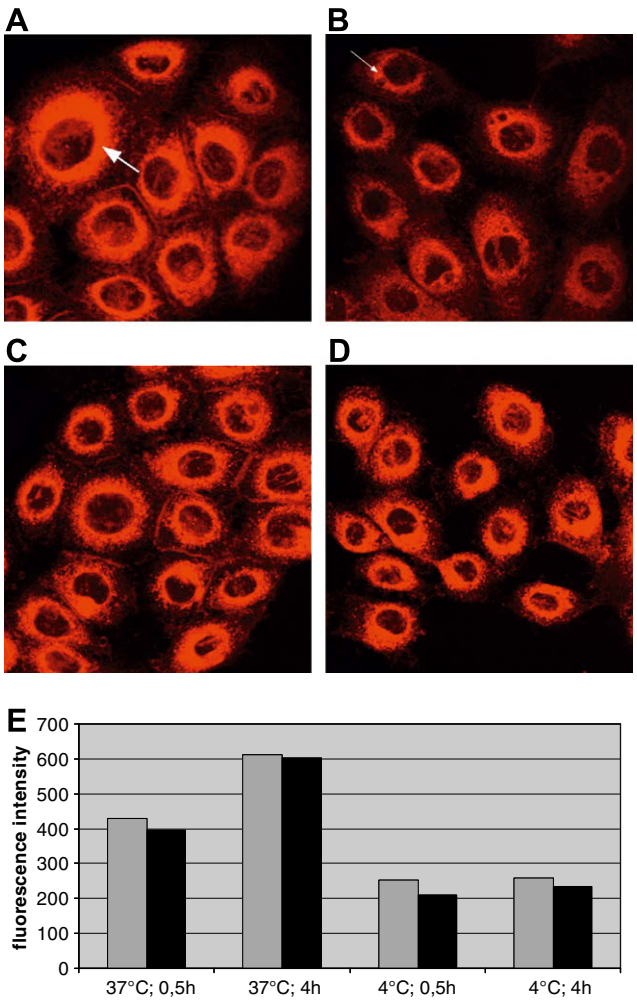

Fig. 6. Endocytotic uptake of SLN (A and C) and CMS nanotransporters (B and D) by keratinocytes after incubation at 37 °C for 0.5 h (A and B) and under energy depletion (C and D) depicted by LSM. White arrows mark endocytotic vesicles. Cellular uptake quantified by a microplate reader shows time and temperature depended uptake (E; SLN, grey columns; CMS nanotransporters, black columns).

dye. In contrast to the dispersions, cream cannot be tested in monolayer cultures.

Incubation at 4 °C did not exclude yet decreases cellular uptake as seen by LSM (data not shown) and ensured by the quantification of the fluorescence in the microplate reader. Fluorescence intensities do not increase from 0.5 to 4 h at 4 °C (Fig. 6E). As monitored by LSM, no decrease of particle uptake was observed with incubation under energy depletion (Fig. 6C and D). The results suggest that partially energy independent processes are involved in the uptake process. And at least partially ATP-independent glycoprotein-related uptake process is also documented for hepatocytes [49] and a fibroblast cell line [50]. Human microvascular endothelial cells internalized dendritic nanotransporters of the Newkome-type by a non-active process, too [51].

Considering cellular uptake by keratinocytes, SLN and CMS nanotransporters do not differ fundamentally from liposomes [43,44]. Cellular uptake of drug-loaded nanoparticles can become clinically relevant when applied to the damaged skin.

4. Conclusions

SLNs as well as dendritic core-multishell nanotransporters are efficient carriers for drug delivery to the skin. Due to the superior ratio of particle surface to volume, small sized CMS nanotransporters were most promising. This mechanism even surmounts the effect of mixing of epidermal lipids and the matrix lipids of SLN, which can facilitate penetration especially of drugs, too. With respect to both wanted benefit and unwanted adverse effects, a major increase of drug concentration within keratinocytes has to be kept in mind, if nanoparticles are applied to the damaged skin.

Acknowledgements

Financial support of the German Research Foundation (FG 463) is gratefully acknowledged. Sarah Küchler is a scholarship holder of the NaFöG program of the city of Berlin.

References

[1] M. Schäfer-Korting, W. Mehnert, H.C. Korting, Lipid nanoparticles for improved topical application of drugs for skin diseases, Adv. Drug Deliv. Rev. 59 (2007) 427–443.
[2] G. Cevc, Lipid vesicles and other colloids as drug carriers on the skin, Adv. Drug Deliv. Rev. 56 (2004) 675–711.
[3] M.J. Choi, H.I. Maibach, Liposomes and niosomes as topical drug delivery systems, Skin Pharmacol. Physiol. 18 (2005) 209–219.
[4] R.H. Müller, M. Radtke, S.A. Wissing, Solid lipid nanoparticles (SLN) and nanostructured lipid carriers (NLC) in cosmetic and dermatological preparations, Adv. Drug Deliv. Rev. 54 (Suppl. 1) (2002) S131–155.
[5] A. Kogan, N. Garti, Microemulsions as transdermal drug delivery vehicles, Adv. Colloid Interface Sci. 123–126 (2006) 369–385.
[6] L.B. Lopes, D.A. Ferreira, D. de Paula, M.T. Garcia, J.A. Thomazini, M.C. Fantini, M.V. Bentley, Reverse hexagonal phase nanodispersion of monoolein and oleic acid for topical delivery of peptides: in vitro and in vivo skin penetration of cyclosporin A, Pharm. Res. 23 (2006) 1332–1342.
[7] J.A. Bouwstra, P.L. Honeywell-Nguyen, Skin structure and mode of action of vesicles, Adv. Drug Deliv. Rev. 54 (Suppl. 1) (2002) S41–S55.
[8] S. Lombardi Borgia, M. Regehly, R. Sivaramakrishnan, W. Mehnert, H.C. Korting, K. Danker, B. Röder, K.D. Kramer, M. Schäfer-Korting, Lipid nanoparticles for skin penetration enhancement-correlation to drug localization within the particle matrix as determined by fluorescence and parelectric spectroscopy, J. Control. Release 110 (2005) 151–163.
[9] J. Stecova, W. Mehnert, T. Blaschke, B. Kleuser, R. Sivaramakrishnan, C.C. Zouboulis, H. Seltmann, H.C. Korting, K.D. Kramer, M. Schäfer-Korting, Cyproterone acetate loading to lipid nanoparticles for topical acne treatment: particle characterisation and skin uptake, Pharm. Res. 24 (2007) 991–1000.
[10] R. Sivaramakrishnan, C. Nakamura, W. Mehnert, H.C. Korting, K.D. Kramer, M. Schäfer-Korting, Glucocorticoid entrapment into lipid carriers – characterisation by parelectric spectroscopy and influence on dermal uptake, J. Control. Release 97 (2004) 493–502.
[11] K.A. Shah, A.A. Date, M.D. Joshi, V.B. Patravale, Solid lipid nanoparticles (SLN) of tretinoin: potential in topical delivery, Int. J. Pharm. 345 (2007) 163–171.
[12] V. Masini, F. Bonte, A. Meybeck, J. Wepierre, Cutaneous bioavailability in hairless rats of tretinoin in liposomes or gel, J. Pharm. Sci. 82 (1993) 17–21.
[13] M. Schäfer-Korting, H.C. Korting, E. Ponce-Pöschl, Liposomal tretinoin for uncomplicated acne vulgaris, Clin. Investig. 72 (1994) 1086–1091.
[14] M. Schäfer-Korting, B. Kleuser, M. Ahmed, H.D. Höltje, H.C. Korting, Glucocorticoids for human skin: new aspects of the mechanism of action, Skin Pharmacol. Physiol. 18 (2005) 103–114.
[15] H. Fesq, J. Lehmann, A. Kontny, I. Erdmann, K. Theiling, M. Rother, J. Ring, G. Cevc, D. Abeck, Improved risk-benefit ratio for topical triamcinolone acetonide in transfersome in comparison with equipotent cream and ointment: a randomized controlled trial, Br. J. Dermatol. 149 (2003) 611–619.
[16] K. Embil, S. Nacht, The Microsponge Delivery System (MDS): a topical delivery system with reduced irritancy incorporating multiple triggering mechanisms for the release of actives, J. Microencapsul. 13 (1996) 575–588.
[17] R.C. Wester, R. Patel, S. Nacht, J. Leyden, J. Melendres, H. Maibach, Controlled release of benzoyl peroxide from a porous microsphere polymeric system can reduce topical irritancy, J. Am. Acad. Dermatol. 24 (1991) 720–726.
[18] M. Hadjikirova, P. Troyanova, M. Simeonova, Nanoparticles as drug carrier system of 5-fluorouracil in local treatment of patients with superficial basal cell carcinoma, J. Buon. 10 (2005) 517–521.
[19] R. Alvarez-Roman, A. Naik, Y.N. Kalia, R.H. Guy, H. Fessi, Enhancement of topical delivery from biodegradable nanoparticles, Pharm. Res. 21 (2004) 1818–1825.
[20] R. Haag, Supramolecular drug-delivery systems based on polymeric core-shell architectures, Angew. Chem. Int. Ed. Engl. 43 (2004) 278–282.
[21] M.R. Radowski, A. Shukla, H. von Berlepsch, C. Bottcher, G. Pickaert, H. Rehage, R. Haag, Supramolecular aggregates of dendritic multishell architectures as universal nanocarriers, Angew. Chem. Int. Ed. Engl. 46 (2007) 1265–1269.
[22] N.A. Stasko, C.B. Johnson, M.H. Schoenfisch, T.A. Johnson, E.L. Holmuhamedov, Cytotoxicity of polypropylenimine dendrimer conjugates on cultured endothelial cells, Biomacromolecules 8 (2007) 3853–3859.

[23] S. Roller, H. Zhou, R. Haag, High-loading polyglycerol supported reagents for Mitsunobu- and acylation-reactions and other useful polyglycerol derivatives, Mol. Divers. 9 (2005) 305–316.
[24] A. Sunder, R. Hanselmann, H. Frey, R. Mülhaupt, Controlled synthesis of hyperbranched polyglycerols by ring-opening multibranching polymerization, Macromolecules 32 (1999) 4240–4246.
[25] M. Schäfer-Korting, U. Bock, A. Gamer, A. Haberland, E. Haltner-Ukomadu, M. Kaca, H. Kamp, M. Kietzmann, H.C. Korting, H.U. Krächter, C.M. Lehr, M. Liebsch, A. Mehling, F. Netzlaff, F. Niedorf, M.K. Rübbelke, U. Schäfer, E. Schmidt, S. Schreiber, K.R. Schröder, H. Spielmann, A. Vuia, Reconstructed human epidermis for skin absorption testing: results of the German prevalidation study, ATLA 34 (2006) 283–294.
[26] A. Gysler, K. Lange, H.C. Korting, M. Schäfer-Korting, Prednicarbate biotransformation in human foreskin keratinocytes and fibroblasts, Pharm. Res. 14 (1997) 793–797.
[27] T. Blaschke, L. Kankate, K.D. Kramer, Structure and dynamics of drug-carrier systems as studied by parelectric spectroscopy, Adv. Drug Deliv. Rev. 59 (2007) 403–410.
[28] M. Schäfer-Korting, U. Bock, W. Diembeck, H.J. Düsing, A. Gamer, E. Haltner-Ukomadu, C. Hoffmann, M. Kaca, H. Kamp, S. Kersen, M. Kietzmann, H.C. Korting, H.U. Krächter, C.M. Lehr, M. Liebsch, A. Mehling, C. Müller-Goymann, F. Netzlaff, F. Niedorf, M.K. Rübbelke, U. Schäfer, E. Schmidt, S. Schreiber, H. Spielmann, A. Vuia, M. Weimer, The use of reconstructed human epidermis for skin absorption testing: results of the validation study, ATLA 36 (2008) 161–187.
[29] B. Stella, V. Marsaud, S. Arpicco, G. Geraud, L. Cattel, P. Couvreur, J.M. Renoir, Biological characterization of folic acid-conjugated poly(H2NPEGCA-co-HDCA) nanoparticles in cellular models, J. Drug Target. 15 (2007) 146–153.
[30] B.M. Magnusson, Y.G. Anissimov, S.E. Cross, M.S. Roberts, Molecular size as the main determinant of solute maximum flux across the skin, J. Invest. Dermatol. 122 (2004) 993–999.
[31] R. Alvarez-Roman, A. Naik, Y.N. Kalia, R.H. Guy, H. Fessi, Skin penetration and distribution of polymeric nanoparticles, J. Control. Release 99 (2004) 53–62.
[32] S. Glasstone, K.J. Laidler, H. Eyring, McGraw-Hill, New York, 1941.
[33] R. Sivaramakrishnan, L. Kankate, H. Niehus, K. Kramer, Parelectric spectroscopy of drug-carrier systems – distribution of carrier masses or activation, Biophys. Chem. 114 (2003) 221–228.
[34] M.R. Lorenz, V. Holzapfel, A. Musyanovych, K. Nothelfer, P. Walther, H. Frank, K. Landfester, H. Schrezenmeier, V. Mailander, Uptake of functionalized, fluorescent-labeled polymeric particles in different cell lines and stem cells, Biomaterials 27 (2006) 2820–2828.
[35] C. Braem, T. Blaschke, G. Panek-Minkin, W. Herrmann, P. Schlupp, T. Paepenmüller, C. Müller-Goyman, W. Mehnert, R. Bittl, M. Schäfer-Korting, K.D. Kramer, Interaction of drug molecules with carrier systems as studied by parelectric spectroscopy and electron spin resonance, J. Control Release 119 (2007) 128–135.
[36] K. Jores, A. Haberland, S. Wartewig, K. Mader, W. Mehnert, Solid lipid nanoparticles (SLN) and oil-loaded SLN studied by spectrofluorometry and Raman spectroscopy, Pharm. Res. 22 (2005) 1887–1897.
[37] S. Wissing, R. Müller, The influence of the crystallinity of lipid nanoparticles on their occlusive properties, Int. J. Pharm. 242 (2002) 377–379.
[38] P.K. Mididoddi, M.A. Repka, Characterization of hot-melt extruded drug delivery systems for onychomycosis, Eur. J. Pharm. Biopharm. 66 (2007) 95–105.
[39] H. Schaefer, F. Watts, J. Brod, B. Illel, in: R.C. Scott, R.H. Guy, J. Hadgraft (Eds.), Prediction of Percutaneous Penetration. Methods, Measurments, Modeling, IBC Techncal Services 1990, pp. 163–173.
[40] R. Toll, U. Jacobi, H. Richter, J. Lademann, H. Schaefer, U. Blume-Peytavi, Penetration profile of microspheres in follicular targeting of terminal hair follicles, J. Invest. Dermatol. 123 (2004) 168–176.
[41] C. Santos Maia, W. Mehnert, M. Schaller, H.C. Korting, A. Gysler, A. Haberland, M. Schäfer-Korting, Drug targeting by solid lipid nanoparticles for dermal use, J. Drug Target. 10 (2002) 489–495.
[42] M.B. Pierre, A.C. Tedesco, J.M. Marchetti, M.V. Bentley, Stratum corneum lipids liposomes for the topical delivery of 5-aminolevulinic acid in photodynamic therapy of skin cancer: preparation and in vitro permeation study, BMC Dermatol. 1 (2001) 5.
[43] M. Schaller, H.C. Korting, M.H. Schmid, Interaction of cultured human keratinocytes with liposomes encapsulating silver sulphadiazine: proof of the uptake of intact vesicles, Br. J. Dermatol. 134 (1996) 445–450.
[44] M. Schaller, R. Wurm, H.C. Korting, Direct evidence for uptake of intact liposomes encapsulating silver sulfadiazine by cultured human keratinocytes based on combined transmission electron microscopy and X-ray microanalysis, Antimicrob. Agents Chemother. 41 (1997) 717–719.
[45] M. Edetsberger, E. Gaubitzer, E. Valic, E. Waigmann, G. Kohler, Detection of nanometer-sized particles in living cells using modern fluorescence fluctuation methods, Biochem. Biophys. Res. Commun. 332 (2005) 109–116.
[46] N.P. Innes, G.R. Ogden, A technique for the study of endocytosis in human oral epithelial cells, Arch. Oral Biol. 44 (1999) 519–523.
[47] A. Miglietta, R. Cavalli, C. Bocca, L. Gabriel, M.R. Gasco, Cellular uptake and cytotoxicity of solid lipid nanospheres (SLN) incorporating doxorubicin or paclitaxel, Int. J. Pharm. 210 (2000) 61–67.
[48] P. Greenspan, S.D. Fowler, Spectrofluorometric studies of the lipid probe, nile red, J. Lipid Res. 26 (1985) 781–789.
[49] B.L. Clarke, P.H. Weigel, Recycling of the asialoglycoprotein receptor in isolated rat hepatocytes. ATP depletion blocks receptor recycling but not a single round of endocytosis, J. Biol. Chem. 260 (1985) 128–133.
[50] P. Ukkonen, J. Saraste, K. Korpela, M. Pesonen, L. Kaariainen, Temperature-dependent internalization of virus glycoproteins in cells infected with a mutant of Semliki Forest virus, EMBO J. 1 (1982) 191–196.
[51] K. Huang, B. Voss, D. Kumar, H.E. Hamm, E. Harth, Dendritic molecular transporters provide control of delivery to intracellular compartments, Bioconjug. Chem. 18 (2007) 403–409.